

Numerical solution for Falkner-Skan flow of hybrid nanofluid with porosity effect

Nurul Musfirah Murad¹, Noraihan Afiqah Rawi^{1*}, Sharidan Shafie¹, and Rahimah Mahat²

¹Department of Mathematical Sciences, Faculty of Science, Universiti Teknologi Malaysia, 81310 UTM Johor Bahru, Johor, Malaysia

²Universiti Kuala Lumpur, Malaysian Institute of Industrial Technology, Persiaran Sinaran Ilmu, 81705 Masai, Johor

*Corresponding author. E-mail: noraihanafiqah@utm.my

Received: Dec. 07, 2020; Accepted: July 03, 2021

Hybrid nanofluid is known to improve heat transfer performance, and its advantages have led to relatively reasonable expectations for their applications. This research considered a moving wedge, namely the Falkner-Skan model, which is well-known in the aerodynamic field. Hybrid nanofluid has been chosen where the dispersion of alumina and copper nanoparticles with water as the base fluid is considered in the unsteady mixed convection flow over moving wedge. By using similarity transformations, the governing equations are converted into ordinary differential equations and then numerically solved using MATLAB bvp4c solver. The increasing values of porosity parameter caused the velocity of hybrid nanofluid to increase. The results also indicated that, the effect of porosity parameter improved the values of skin friction coefficient but decrease the value of Nusselt number.

Keywords: Falkner-Skan flow; Unsteady flow; Hybrid nanofluid; Porous medium

© The Author(s). This is an open access article distributed under the terms of the [Creative Commons Attribution License \(CC BY 4.0\)](https://creativecommons.org/licenses/by/4.0/), which permits unrestricted use, distribution, and reproduction in any medium, provided the original author and source are cited.

[http://dx.doi.org/10.6180/jase.202206_25\(3\).0012](http://dx.doi.org/10.6180/jase.202206_25(3).0012)

1. Introduction

After nanofluid has been studied in various aspects, hybrid nanofluid is introduced, and many researchers studied this new fluid because of its applications practically in all fields such as medical, acoustic, microfluid, micro-electrical, manufacturing, naval structures, transportation, etc. Hybrid nanofluid is produced by the dispersing of two various types of nanoparticles in the base fluid. The significance of nanomaterials' composition was chosen to magnify each other's useful compatible features. Alumina is one of the potential nanoparticles among researchers in previous findings because of its good deal with stability and chemical motionlessness, even though its thermal conductivity towards metal nanoparticles is low [1, 2].

Zinc, silver, copper, and aluminium are other metal nanoparticles which have an outstanding thermal conductivity. Previous studies have proved an appropriate im-

provement through hybrid nanofluids by Sarkar et al. [3]. Related papers and articles on hybrid nanofluids can be observed in [4–11].

Some related research involved fluid loading in a porous medium with porosity and permeability can be referred in [12–16]. Porosity can be defined as the fraction of void volume over the total volume, play a significant role in geology due to the management of fluid storage in aquifers, oil, and gas fields. Chandrasekhara and Namboudiri [17] analyzed forced and free convection flows in a porous medium with variable permeability. Rees and Pop [18] explored free convection through porous medium together with permeability. Saif et al. [19] presented fluid flow over a porous medium with thermal conductivity and porosity.

Studies on various convective boundary layer flow past different types of geometries have been conducted in various aspects. The most frequent study has been the wedge flow, where it can be static or moving with different or

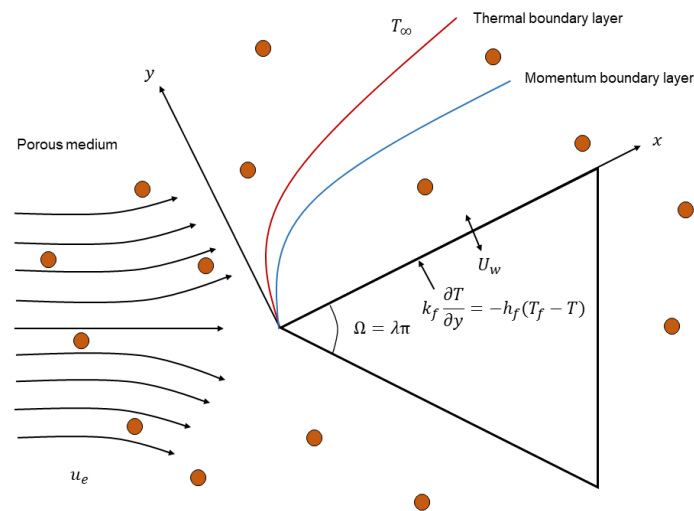


Fig. 1. Physical model and coordinate system

same fluid direction. Falkner and Skan [20] was the earliest one who proposed the wedge flow and named it after their name. The Falkner-Skan flow is well-known in the aerodynamic field. Some of the applications that we can apply in real life are the bow of a ship, the wingtip of an airplane, and a Formula One car's shape. They developed a model that is not parallel to flow direction based on the boundary layer theory. Watanabe [21] investigated the thermal boundary layer in the presence of injection or suction over a wedge with uniform force flow.

Kumari et al. [22] examined mixed convection flow through a vertical wedge embedded in a porous medium. Then, Ishak et al. [23] explored the unsteady mixed convection boundary layer flow using the Falkner-Skan model with heat generation in the presence of injection or suction. Ganapathirao et al. [24] studied the Falkner-Skan equation with the presence of injection or suction. Ullah et al. [25] studied the mixed convection flow of Casson fluid with the Falkner-Skan model with heat transfer.

Despite all the papers published, the unsteady Falkner-Skan flow of hybrid nanofluid over a moving wedge with the effect of porosity has never been explored. Inspired by this developing movement of hybrid nanofluid, an attempt is made to investigate the unsteady Falkner-Skan flow of hybrid nanofluid, a dispersion of copper and alumina with water base fluid through a moving wedge.

2. Materials and methods

Two-dimensional mixed convection unsteady flow of hybrid nanofluid over a porous medium is considered. In this problem, the wedge is moving with the velocity $U_w =$

$\frac{ax^m}{(1-\varepsilon t)^{\frac{1}{2}}}$ and the free stream velocity $u_e = \frac{bx^m}{(1-\varepsilon t)^{\frac{1}{2}}}$, where a and b are constants. The hybrid nanofluid considered a no-slip condition that transpires between them and in thermal equilibrium. The fluid flow is utilized at $x, y \geq 0$, where x -axis is taken along the wedge's surface while the y -axis is familiar to the x -axis in the outward direction towards the fluid.

Here, $\lambda = \frac{\Omega}{\pi}$ is the sum of angle Ω of the wedge equivalent to $\lambda = \frac{2m}{(m+1)}$, the Hartree pressure gradient parameter where m is angle wedge parameter (see Fig. 1). Also, the temperature, T , considered at the wedge and heated at the temperature $T_f = T_\infty + \frac{T_0 x^{2m-1}}{(1-\varepsilon t)^2}$, T_0 are constants and the temperature in the ambient fluid as T_∞ . A water-based hybrid nanofluid that will be characterized in this research is composite hybrid nanoparticles of copper (Cu) and alumina (Al_2O_3).

The volume of solid fraction for Cu and Al_2O_3 nanoparticles, are taken as $\phi_1 = \phi_2 = 0.1$, referred in [4].

The hybrid nanofluid's thermophysical attributes are referred to in Table 1.

The governing equations of unsteady Falkner-Skan flow of a hybrid nanofluid can be written as follows [4, 25, 26],

$$\frac{\partial u}{\partial x} + \frac{\partial v}{\partial y} = 0 \quad (1)$$

$$\begin{aligned} \frac{\partial u}{\partial t} + u \frac{\partial u}{\partial x} + v \frac{\partial v}{\partial y} &= \frac{\partial u_e}{\partial t} + u_e \frac{\partial u_e}{\partial x} \\ &+ \frac{\mu_{hmf}}{\rho_{hmf}} \frac{\partial^2 u}{\partial y^2} + \frac{\varphi \mu_{hmf}}{k_1 \rho_{hmf}} (u_e - u) \end{aligned} \quad (2)$$

$$\frac{\partial T}{\partial t} + u \frac{\partial T}{\partial x} + v \frac{\partial T}{\partial y} = \alpha_{hmf} \frac{\partial^2 T}{\partial y^2} \quad (3)$$

Table 1. The thermophysical properties of nanoparticles and base fluid referred in [4]

Thermophysical properties	Thermal conductivity k(W/mK)	Specific heat C _p (J/kgK)	Density ρ(kg/m ³)
Copper (Cu)	400	385	8933
Alumina (Al ₂ O ₃)	40	765	3970
Water	0.613	4179	997.1

subject to the following boundary conditions [27],

$$\begin{aligned}
 u &= U_w = \frac{ax^m}{(1-\varepsilon t)^{\frac{1}{2}}}, v = 0, \\
 -k_f \frac{\partial T}{\partial y} &= h_f (T_f - T) \text{ at } y = 0 \\
 u &= u_e = \frac{bx^m}{(1-\varepsilon t)^{\frac{1}{2}}}, T \rightarrow T_\infty \text{ when } y \rightarrow \infty
 \end{aligned} \tag{4}$$

Where, u and v are the velocity components together with x and y directions, ρ_{hnf} , α_{hnf} , μ_{hnf} , are density, thermal diffusivity and viscosity of hybrid nanofluid, respectively, k_1 is the permeability of the porous medium, φ is the porosity, $k_f = \frac{k_0(1-\varepsilon t)}{x^{m-1}}$ is the thermal conductivity of the fluid and $h_f = \frac{h_0 x^{\frac{m-1}{2}}}{(1-\varepsilon t)^{\frac{1}{2}}}$ is the convective heat transfer where k_0 and h_0 are constants.

The similarity transformations are introduced [25],

$$\begin{aligned}
 \eta &= y \sqrt{\frac{u_e(1+m)}{2xv_f(1-\varepsilon t)}}, \\
 \psi &= \sqrt{\frac{2xv_f u_e}{(1+m)(1-\varepsilon t)}} f(\eta), \\
 \theta(\eta) &= \frac{T - T_\infty}{T_f - T_\infty}
 \end{aligned} \tag{5}$$

Where the stream function, ψ is defined by the following relations,

$$u = \frac{\partial \psi}{\partial y}, v = -\frac{\partial \psi}{\partial x} \tag{6}$$

The governing equations (2) and (3) are transformed into ordinary differential equations as follows,

$$\begin{aligned}
 &\frac{\mu_{hnf} \rho_f}{\rho_{hnf} \mu_f} f'''(\eta) + f(\eta) f''(\eta) \\
 &+ \lambda (1 - f'(\eta)^2) + K (1 - f'(\eta)) \\
 -A &\left[\frac{2}{m+1} f'(\eta) + \frac{1}{m+1} \eta f''(\eta) - \frac{2}{m+1} \right] = 0 \\
 &\frac{1}{Pr} \frac{\alpha_{hnf}}{\alpha_f} \theta''(\eta) + f(\eta) \theta'(\eta) - 2\lambda f'(\eta) \theta(\eta) \\
 -A &\left[\frac{4m}{m+1} \theta(\eta) + \frac{1}{m+1} \eta \theta'(\eta) \right] = 0
 \end{aligned} \tag{7}$$

subject to the following transformed boundary conditions,

$$\begin{aligned}
 f(\eta) &= 0, f'(\eta) = \gamma, \theta'(\eta) = \\
 &-\sqrt{\frac{2}{m+1}} Bi(1 - \theta(\eta)) \text{ at } \eta = 0 \\
 f'(\eta) &\rightarrow 1, \theta(\eta) \rightarrow 0 \text{ when } \eta \rightarrow \infty
 \end{aligned} \tag{9}$$

Where,

$$\begin{aligned}
 \gamma &= \frac{U_w}{u_e}, K = \frac{2x\varphi\mu_{hnf}}{u_e(m+1)k_1\rho_{hnf}}, Pr = \frac{v_f}{\alpha_f}, \\
 A &= \frac{\varepsilon}{1-\varepsilon t} \frac{x}{u_e}, Bi = \frac{h_f}{k_f} Re_x^{-\frac{1}{2}}, Re_x = \frac{Ux}{v_f}
 \end{aligned} \tag{10}$$

Here γ is the moving wedge parameter, K is the porosity parameter, Pr is the Prandtl number, A is an unsteady parameter, Bi is Biot number and Re_x is Reynold's number. The critical physical quantities of this problem are skin friction coefficient Cf_x and the local Nusselt number Nu_x are obtained as follows,

$$\begin{aligned}
 (Re_x)^{\frac{1}{2}} Cf_x &= \sqrt{\frac{(m+1)}{2}} \frac{\mu_{hnf}}{\mu_f} f''(0), \\
 (Re_x)^{-\frac{1}{2}} Nu_x &= -\sqrt{\frac{(m+1)}{2}} \frac{k_{hnf}}{k_f} \theta'(0)
 \end{aligned} \tag{11}$$

The system of equations (7) and (8), together with the transformed boundary conditions (9), are solved by using MATLAB bvp4c solver. To generate the coding, the transformed governing equations need to convert into the system of first-order equations. The first-order linear differential equations and the transformed boundary conditions will then be coded in MATLAB to run the solver. Finally, the numerical results will be graphically analyzed.

3. Results and Discussion

The results on velocity, $f'(\eta)$, and temperature profiles, $\theta(\eta)$ for unsteady parameter, A , porosity parameter, K , angle wedge parameter, m , and moving wedge parameter, γ are presented. The validation of the present results is checked by comparing the results with the earlier literature results, as indicated in Table 2 The present results of local skin friction coefficient with distinct values of m together with the results of Watanabe [21], Kumari et al. [22], Ishak et al. [23], Ganapathirao et al. [24], Ullah et al. [25], are found in an excellent deal. It can also be observed that

Table 2. Skin friction coefficient for different values of m with $Pr = 0.73, K = A = \gamma = 0$, where $\lambda = 2m/(m + 1)$

m	Watanabe (difference-differential method) [21]	Kumari et al. (Keller box method) [22]	Ishak et al. (Keller box method) [23]	Ganapathirao et al. (Implicit finite difference scheme) [24]	Ullah et al. (Keller box method) [25]	Present results
0	0.46960	0.46975	0.4696	0.46972	0.4696	0.46960
0.0141	-	0.50472	0.5046	0.50481	0.5046	0.50462
0.0435	0.56898	0.56904	0.5690	0.56890	0.5690	0.56898
0.0909	0.65498	0.65501	0.6550	0.65493	0.6550	0.65498
0.1429	0.73200	0.73202	0.7320	0.73196	0.7320	0.73200
0.2000	0.80213	0.80214	0.8021	0.80215	0.8021	0.80213
0.3333	0.92765	0.92766	0.9277	0.92767	0.9277	0.92766

the local friction coefficient increases with an increase of m , which leads to the resistant force exerted on a moving wedge in a fluid. In other words, drag force or skin friction coefficient slow the movement of any objects.

Table 3. Numerical results of skin friction coefficient and Nusselt number for various values of A, m, K and γ .

A	m	K	γ	$(Re_x)^{\frac{1}{2}} C_{f_x}$	$(Re_x)^{\frac{1}{2}} Nu_x$	
0.2	0.25	0.6	0.3	1.5831	0.3254	
0.4				1.6681	0.3780	
0.8				1.8288	0.4436	
	0.2857	0.8	0.3	1.6314	0.3189	
				0.8	2.2072	0.3263
				1.5	1.6614	0.3247
			1.5	1.9056	0.3227	
			0	2.0323	0.3374	
			-0.3	2.3453	0.3504	

Fig. 2 represents the effect of the unsteady parameter, A , with three different values of K , where $K = 0$ corresponds to the non-porous medium, and $K \neq 0$ corresponds to the porous medium. It is revealed that $f'(\eta)$ increase with the increment in A , while the dimensionless temperature falls due to the distance between the molecules, become more significant in the unsteady flow. This leads to an improvement in the rate of cooling of the fluid. Thus, the unsteady parameter must be well-considered and highlighted for the practical matter. It is observed that the fluid flow temperature over a porous medium is higher than the fluid flow temperature over a non-porous medium. Porosity influence the convection flows frequently, and, as an outcome, the fluid velocity increase.

Fig. 3 illustrates the effect of moving wedge parameter, γ on $f'(\eta)$ and $\theta(\eta)$ for various values of K . Three different cases are considered where $\gamma < 0$ is the wedge moves in the opposite direction to the fluid motion, $\gamma = 0$ is the wedge is static or stationary, and $\gamma > 0$ is the wedge moves in the same direction with the fluid motion. The velocity profiles

rise with the increasing values of γ . It is observed that in all cases of γ , when porosity increases, the temperature increases and slowly decreases. Note that the permeability's effect decreases the boundary layer thickness, which plays the same role as the pressure gradient on the boundary layer.

Table 3 represent the influences of governing parameters on the variation of skin friction coefficient and Nusselt number. It is observed that the skin friction coefficient increase when A, K, m increase and γ decreases. As for the Nusselt number, it fluctuates when m increase. It is also shown that the Nusselt number increase when A increases and γ decrease. Besides, it is observed that the Nusselt number decreases with the increasing value of K .

4. Conclusion

The unsteady hybrid nanofluid with the effect of porosity is numerically studied over a moving wedge. The highlighted results are given as follows:

1. Hybrid nanofluid flow increases with the rise of the A, K , and γ ,
2. The temperature distribution reduces with the increment of A but rises with the increment of K, γ then slowly to decrease,
3. An increase in K increases the skin friction coefficient but decreases the Nusselt number.
4. For small K , an increase in interfacial heat transfer area will enhance heat transfer between phases and reduce the duration of time necessary to reach thermal equilibrium.

Acknowledgment

The authors would like to acknowledge the Research Management Centre, UTM, Center for Research and Innova-

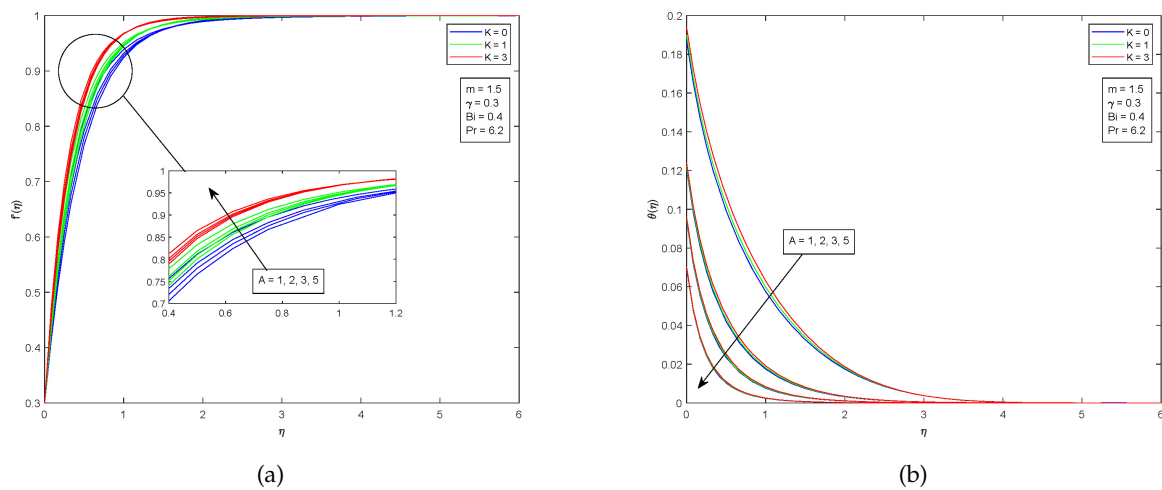


Fig. 2. The effect of A on velocity and temperature profiles for different values of K .

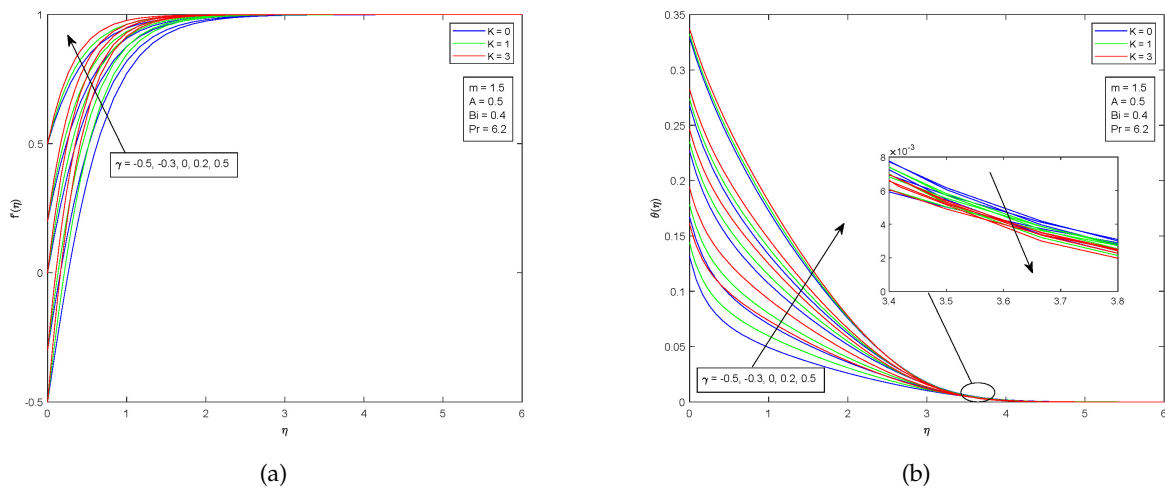


Fig. 3. The effect of γ on velocity and temperature profiles for different values of K .

tion, UniKL, and Ministry of Higher Education (MOHE), Malaysia, the financial support through vote numbers, 08G33, FRGS/ 1 / 2018 / STG06 / UTM/ 02 / 4, FRGS / 1 / 2019 / STG06 / UTM / 02 / 22, and FRGS / 1 / 2019 / STG06 / UNIKL / 03 / 1 for this research.

References

- [1] M. Salem Ahmed, M. R. A. Hady, and G. Abdallah, (2018) "Experimental investigation on the performance of chilled-water air conditioning unit using alumina nanofluids" **Thermal Science and Engineering Progress** 5: 589–596. DOI: <https://doi.org/10.1016/j.tsep.2017.07.002>.
- [2] M. S. Ahmed and A. M. Elsaid, (2019) "Effect of hybrid and single nanofluids on the performance characteristics of chilled water air conditioning system" **Applied Thermal Engineering** 163: 114398. DOI: <https://doi.org/10.1016/j.applthermaleng.2019.114398>.
- [3] J. Sarkar, P. Ghosh, and A. Adil, (2015) "A review on hybrid nanofluids: Recent research, development and applications" **Renewable and Sustainable Energy Reviews** 43: 164–177. DOI: <https://doi.org/10.1016/j.rser.2014.11.023>.
- [4] N. A. L. Aladdin, N. Bachok, and I. Pop, (2020) "Cu-Al₂O₃/water hybrid nanofluid flow over a permeable moving surface in presence of hydromagnetic and suction effects" **Alexandria Engineering Journal** 59(2): 657–666. DOI: <https://doi.org/10.1016/j.aej.2020.01.028>.

- [5] I. Waini, A. Ishak, and I. Pop, (2019) "Hybrid nanofluid flow and heat transfer over a nonlinear permeable stretching/shrinking surface" **International Journal of Numerical Methods for Heat & Fluid Flow**:
- [6] T. Hayat and S. Nadeem, (2017) "Heat transfer enhancement with Ag-CuO/water hybrid nanofluid" **Results in Physics** 7: 2317–2324. DOI: <https://doi.org/10.1016/j.rinp.2017.06.034>.
- [7] S. Ghadikolaei, M. Yassari, H. Sadeghi, K. Hosseinzadeh, and D. Ganji, (2017) "Investigation on thermophysical properties of Tio2-Cu/H2O hybrid nanofluid transport dependent on shape factor in MHD stagnation point flow" **Powder Technology** 322: 428–438. DOI: <https://doi.org/10.1016/j.powtec.2017.09.006>.
- [8] B. M. Al-Srayyih, S. Gao, and S. H. Hussain, (2019) "Natural convection flow of a hybrid nanofluid in a square enclosure partially filled with a porous medium using a thermal non-equilibrium model" **Physics of Fluids** 31(4): 043609.
- [9] M. Usman, M. Hamid, T. Zubair, R. Ul Haq, and W. Wang, (2018) "Cu-Al2O3/Water hybrid nanofluid through a permeable surface in the presence of nonlinear radiation and variable thermal conductivity via LSM" **International Journal of Heat and Mass Transfer** 126: 1347–1356. DOI: <https://doi.org/10.1016/j.ijheatmasstransfer.2018.06.005>.
- [10] M. Izadi, R. Mohebbi, D. Karimi, and M. A. Sheremet, (2018) "Numerical simulation of natural convection heat transfer inside a \perp shaped cavity filled by a MWCNT-Fe3O4/water hybrid nanofluids using LBM" **Chemical Engineering and Processing - Process Intensification** 125: 56–66. DOI: <https://doi.org/10.1016/j.cep.2018.01.004>.
- [11] M. Ghalambaz, M. A. Sheremet, S. Mehryan, F. M. Kashkooli, and I. Pop, (2019) "Local thermal non-equilibrium analysis of conjugate free convection within a porous enclosure occupied with Ag-MgO hybrid nanofluid" **Journal of Thermal Analysis and Calorimetry** 135(2): 1381–1398.
- [12] M. Adil Sadiq and T. Hayat, (2016) "Darcy-Forchheimer flow of magneto Maxwell liquid bounded by convectively heated sheet" **Results in Physics** 6: 884–890. DOI: <https://doi.org/10.1016/j.rinp.2016.10.019>.
- [13] J. Umavathi, O. Ojjela, and K. Vajravelu, (2017) "Numerical analysis of natural convective flow and heat transfer of nanofluids in a vertical rectangular duct using Darcy-Forchheimer-Brinkman model" **International Journal of Thermal Sciences** 111: 511–524. DOI: <https://doi.org/10.1016/j.ijthermalsci.2016.10.002>.
- [14] T. Hayat, A. Aziz, T. Muhammad, and A. Alsaedi, (2018) "An optimal analysis for Darcy-Forchheimer 3D flow of nanofluid with convective condition and homogeneous-heterogeneous reactions" **Physics Letters A** 382(39): 2846–2855. DOI: <https://doi.org/10.1016/j.physleta.2018.06.015>.
- [15] A. K. Alzahrani, (2018) "Darcy-Forchheimer 3D flow of carbon nanotubes with homogeneous and heterogeneous reactions" **Physics Letters A** 382(38): 2787–2793. DOI: <https://doi.org/10.1016/j.physleta.2018.06.011>.
- [16] Z. Shah, A. Dawar, S. Islam, I. Khan, and D. L. C. Ching, (2018) "Darcy-Forchheimer flow of radiative carbon nanotubes with microstructure and inertial characteristics in the rotating frame" **Case Studies in Thermal Engineering** 12: 823–832. DOI: <https://doi.org/10.1016/j.csite.2018.09.007>.
- [17] B. Chandrasekhara and P. Namboodiri, (1985) "Influence of variable permeability on combined free and forced convection about inclined surfaces in porous media" **International Journal of Heat and Mass Transfer** 28(1): 199–206. DOI: [https://doi.org/10.1016/0017-9310\(85\)90022-5](https://doi.org/10.1016/0017-9310(85)90022-5).
- [18] D. Rees and I. Pop, (2000) "Vertical free convection in a porous medium with variable permeability effects" **International Journal of Heat and Mass Transfer** 43(14): 2565–2571. DOI: [https://doi.org/10.1016/S0017-9310\(99\)00316-6](https://doi.org/10.1016/S0017-9310(99)00316-6).
- [19] R. S. Saif, T. Muhammad, and H. Sadia, (2020) "Significance of inclined magnetic field in Darcy-Forchheimer flow with variable porosity and thermal conductivity" **Physica A: Statistical Mechanics and its Applications** 551: 124067. DOI: <https://doi.org/10.1016/j.physa.2019.124067>.
- [20] V. Falkner and S. Skan, (1931) "Some approximate solutions of the boundary-layer for flow past a stretching boundary" **SIAM J Appl Math** 49: 1350–1358.
- [21] T. Watanabe, (1990) "Thermal boundary layers over a wedge with uniform suction or injection in forced flow" **Acta Mechanica** 83(3): 119–126.
- [22] M. Kumari, H. S. Takhar, and G. Nath, (2001) "Mixed convection flow over a vertical wedge embedded in a highly porous medium" **Heat and Mass Transfer** 37(2): 139–146.

- [23] A. Ishak, R. Nazar, and I. Pop, (2007) "Falkner-Skan equation for flow past a moving wedge with suction or injection" **Journal of Applied Mathematics and Computing** 25(1): 67–83.
- [24] M. Ganapathirao, R. Ravindran, and E. Momoniat, (2015) "Effects of chemical reaction, heat and mass transfer on an unsteady mixed convection boundary layer flow over a wedge with heat generation/absorption in the presence of suction or injection" **Heat and Mass Transfer** 51(2): 289–300.
- [25] I. Ullah, I. Khan, and S. Shafie, (2016) "Hydromagnetic Falkner-Skan flow of Casson fluid past a moving wedge with heat transfer" **Alexandria Engineering Journal** 55(3): 2139–2148. DOI: <https://doi.org/10.1016/j.aej.2016.06.023>.
- [26] I. Ullah, S. Shafie, O. D. Makinde, and I. Khan, (2017) "Unsteady MHD Falkner-Skan flow of Casson nanofluid with generative/destructive chemical reaction" **Chemical Engineering Science** 172: 694–706. DOI: <https://doi.org/10.1016/j.ces.2017.07.011>.
- [27] I. Ullah, S. Shafie, and I. Khan, (2017) "MHD Mixed convection flow of Casson fluid over a moving wedge saturated in a porous medium in the presence of chemical reaction and convective boundary conditions" **Journal of Science and Technology** 9(3):